ISSN 1075-7015, Geology of Ore Deposits, 2006, Vol. 48, No. 5, pp. 357–368. © Pleiades Publishing, Inc., 2006.
Original Russian Text © T.S. Livshits, 2006, published in Geologiya Rudnykh Mestorozhdenii, 2006, Vol. 48, No. 5, pp. 410–422.

Britholites As Natural Analogues of Actinide Matrices: Resistance to Radiation Damage

T. S. Livshits

Institute of Geology of Ore Deposits, Petrography, Mineralogy, and Geochemistry, Russian Academy of Sciences, Staromonetnyi per. 35, Moscow, 119017 Russia

Received June 14, 2006

Abstract—Crystallization of borosilicate glasses, used now for solidification of liquid nuclear high-level wastes (HLW), is accompanied by the formation of silicates with the apatite-type structure and high contents of actinides and REE. The stability of these silicates determines the safety of immobilization of radionuclides. As a result of radioactive decay, the crystalline phases of actinides become amorphous with time and their solubility in aqueous solutions increases. One of the ways to assess the radiation stability of compounds is the study of their natural analogues that contain radioactive elements. Minerals of the britholite group are the natural analogues of synthetic rare earth silicates and actinides with the apatite-type structure. Seven britholites of different ages and with different $ThO_2 + UO_2$ contents have been studied. The stages of partial damage and complete destruction of sample structures under the effect of radioactive decay were distinguished. The radiation stability of natural britholites surpasses that of their synthetic analogues. The annealing of metamict samples recovers the primary apatite-type structure without formation of any other phases. With an increase in annealing duration from 1 to 5 h, the mineral structure is recovered at a lower (by 200°C) temperature (down to 550–600°C). The temperature conditions in underground storages and the substantially longer occurrence of HLW therein will prevent crystalline matrices with the apatite-type structure from amorphization and thus ensure the retention of their stability.

DOI: 10.1134/S1075701506050023

INTRODUCTION

At present, the liquid high-level wastes (HLW) of the nuclear fuel cycle are immobilized by incorporation into aluminum phosphate (*Phosphate Glasses*…, 1997) or borosilicate (Sombret, 1987) glasses. The heat release related to the decay of radioactive isotopes promotes glass crystallization. The study of borosilicate glasses has shown that their devitrification is accompanied by the formation of silicate crystalline phases with the apatite-type structure ($P6_3/m$, $Z = 2$) that are able to incorporate significant quantities of actinides and REE contained in HLW (Zhao et al., 2001; Rose et al., 2004). This is evident, in particular, from the REE distribution between glass and silicate with the apatite-type structure (Smelova et al., 2000). It has been shown that the crystalline phase is substantially enriched in La, Ce, Nd, and Eu in comparison with the glass. Actinides (Np, Pu, Am, and Cm) close in the size of ions and their charges to REE should behave in a similar way. Data on minerals of the britholite group, natural analogues of such synthetic phases, also indicate their high isomorphic capacity with respect to actinides and REE. The $ThO_2 + UO_2$ and REE_2O_3 contents in britholites amount to 23 and 63 wt %, respectively (Kupriyanova et al., 1966).

Corresponding author: T.S. Livshits. E-mail: lita_239@yahoo.com

The interest in phases with the apatite-type structure is also explained by the search for alternative matrices for actinide HLW. Glass ceramics containing from 20 to 50% crystalline phases incorporated into glass (Sombret, 1987) serve as examples of such matrices. Crystalline phases, including ones with the apatite-type structure, ensure immobilization of actinides (Zhao et al., 2001).

The chemical stability of crystalline phases is substantially higher as compared with that of glass. Some of these phases are resistant to aqueous solutions (Ewing, 2001; Lumpkin, 2001). It may be suggested that incorporation of HLW components into matrices based on synthetic analogues of such minerals will provide reliable fixation of radionuclides and prevent their migration during long-term storage.

The radiation stability of crystalline phases, an important parameter that characterizes their capacity to immobilize radioactive isotopes, is determined by the critical irradiation dose that gives rise to a transition to the metamict state and by the critical temperature at which amorphization does not occur at any irradiation dose. The critical dose is established by irradiation of synthetic compounds by ions of heavy elements (for example, noble gases), by implantation of short-lived isotopes (^{244}Cm, ^{238}Pu) into the phase structure, and by studying natural U- and Th-bearing mineral analogues

(Ewing et al., 1995). The critical temperature is determined with the first two methods only.

The radiation stability of phases with the apatite-type structure has been studied mainly with heavy ion irradiation and implantation of short-lived ions (Weber and Ewing, 2002; Utsunomiya et al., 2003). A wide range of critical irradiation doses has been obtained. Therefore, it is an important task to refine this parameter based on the study of minerals of the britholite group as natural radioactive analogues of these compounds.

In order to trace successive stages of structural destruction of natural samples under the effect of radioactive decay and to determine their radiation stability, it is necessary to examine minerals of different ages and with different contents of radioactive elements. Such minerals are characterized by different degrees of structure retention, allowing assessment of the accumulated irradiation dose leading to amorphization of the lattice. The difficulties related to the study of natural britholites are due to the fact that these minerals usually occur in the X-ray amorphous state.

This paper presents the results of study of britholites characterized by different age and different ThO_2 and UO_2 contents. The radiation stability of these phases has been assessed, and recrystallization of amorphous samples by annealing has been investigated.

RESEARCH METHODS

Seven britholite samples from alkaline rocks of Russia were chosen for this study. Their age was estimated at 26×10^8 yr in the West Keivy Massif, Kola Peninsula (Belyaev et al., 2001), 15.0×10^8 yr in the Mariupol Massif, Azov region (Nechaev and Krivdyuk, 1989), 3.2×10^8 yr in the Burpala Massif, East Siberia (Zhidkov et al., 1963), and 3.0×10^8 yr at the Sol'sky deposit, Buryatia (Chuprov, 1972).

The structure of samples was studied with XRD on a Rigaku D/Max 2200 diffractometer (CuK_α radiation, voltage 40 keV, current 20–30 mA, 2θ angular range from 20° to 70°, measurement step 0.01°–0.02°). When interpreting X-ray patterns, the PCPDF database (JCPDS–ICDD, 1997–1999) was used. The sample structure was also studied with a JEM-100 C TEM (resolution 7 Å and accelerating voltage 100 keV).

The compositions of samples were determined with a JSM-5300 SEM equipped with a Link ISIS energy dispersive analyzer (voltage 25 keV; current 1 nA; diameter of the analyzed zone 1–3 μm; pulse collection time 100 s; metals, oxides, and fluorides were used as reference samples).

To recover the structure, four metamict samples were annealed at 750°C for 6 h. The dynamics of this process was studied more thoroughly with DTA on a Derivatograph device at an annealing rate of 10°/min. To study recrystallization, one metamict sample was heat treated at temperatures of 100 and 300°C for 7 h; 500, 550, 600, 700, and 800°C for 5 h; and 500°C for 8 h.

CHARACTERISTICS OF THE STUDIED NATURAL BRITHOLITE SAMPLES

Chemical compositions. Based on the SEM data (Table 1) and in line with the classification of minerals from the britholite group (Kupriyanova et al., 1966), it was established that samples 1771, 65863, 1769, and Bt-8 are britholites proper ($ThO_2 < 10\%$, $Al_2O_3 < 5\%$, ΣCeREE > ΣYREE); sample 89510 is classed with spencite ($ThO_2 < 10\%$, $Al_2O_3 < 5\%$, ΣCeREE < ΣYREE, $P_2O_5 \approx 0$); and samples 1775 and 62388 pertain to fenghuanglite, or Th-britholite ($ThO_2 > 10\%$, $Al_2O_3 < 5\%$, ΣCeREE > ΣYREE). All these minerals, except spencite in sample 89510, contain from 1.8 to 5.2 wt % F^-. Totals in all analyses, except samples 1769 and 62388, are notably below 100%. This is probably explained by occurrence in minerals of water (as H_2O and OH^-) and B_2O_3. These components are not detectable by applied analytical methods. According to (Kupriyanova et al., 1966), the H_2O and B_2O_3 contents in britholites may be as high as 11–12 wt %. Recalculation of chemical compositions of samples to their formulas shows that the contents of the apatite $[Ca_{10}(PO_4)_6F_2]$ and britholite $[Ca_4(REE,Ln)_6(SiO_4)_6O]$ end members range within 12–19 and 81–88%, respectively. The sole exception is spencite in sample 89510, which is devoid of phosphorus and, hence, does not have an apatite component in its formula.

The SEM study revealed different compositions of samples (Table 2). BSE images (Fig. 1) demonstrate that all britholites are characterized by a zonal or mosaic (spotty) structure. Numerous fractures are observable in samples 1771, 89510, and 62388. A system of small (up to 50 μm long) parallel fractures is observed in the first of these samples. Compositionally different zones up to 10 μm wide (light) and 26 μm wide (dark) are oriented along this system. The study of the chemical composition shows that the zonal patterns of the mineral are controlled by variations in CaO and P_2O_5 contents.

A grain from sample 89510 examined with SEM/EDS is an intergrowth of spencite with yttrialite and thorite. The spencite surface is covered with cracks and related compositionally different bands approximately 10–15 μm wide. The zoning of the mineral is largely determined by variations in CaO and SiO_2 contents.

Sample 62388 contains extended areas up to 100–200 μm long that differ in composition from the groundmass, which are also confined to fractures. The differences in CaO and ThO_2 contents are the most prominent. In addition, small fractures up to 50 μm long and up to 1 μm wide are filled with ThO_2. Such fractures are located in areas depleted in Th and indicate redistribution of this element in the course of britholite alteration.

Table 1. Chemical compositions of samples (SEM/EDS data), wt %

Component	65863[1]	1769[2]	Bt-8[1]	89510[3]	1775[2]	1771[3]	62388[4]
F^-	2.0	5.2	3.7	2.3	1.9	1.8	3.0
SiO_2	20.4	21.4	18.8	21.5	20.5	19.4	22.1
P_2O_5	4.9	5.8	3.0	n.d.	3.3	3.5	3.4
Al_2O_3	n.d.	n.d.	n.d.	0.9	n.d.	n.d.	n.d.
MnO	″	″	″	1.2	″	″	″
FeO	″	″	″	0.8	″	″	″
CaO	15.6	18.6	15.3	15.9	17.0	16.8	19.0
Y_2O_3	1.2	1.8	1.3	30.3	0.8	6.0	n.d.
La_2O_3	15.5	12.3	9.6	1.5	12.1	6.5	12.3
Ce_2O_3	21.7	33.3	25.0	3.7	18.5	17.7	20.9
Pr_2O_3	1.1	n.d.	1.6	0.8	1.2	1.5	1.2
Nd_2O_3	3.6	″	9.8	1.6	4.1	10.3	3.5
Sm_2O_3	n.d.	″	0.9	n.d.	0.8	1.3	n.d.
Eu_2O_3	″	″	0.4	″	n.d.	n.d.	″
Dy_2O_3	″	″	n.d.	2.9	″	″	″
Er_2O_3	″	″	″	2.8	″	″	″
ThO_2	2.0	1.3	4.1	1.2	11.1	4.3	13.8
UO_2	0.2	0.6	0.3	n.d.	0.8	0.6	n.d.
Σ	88.2	100.3	93.8	87.4	92.1	89.7	99.2

Notes: Here and hereafter, n.d. means not detected. [1] Burpala Massif, northern Baikal region. [2] Mariupol Massif, Azov region. [3] West Keivy Massif, Kola Peninsula. [4] Sol'sky deposit, Buryatia.

Table 2. Compositions of differently colored zones in britholite samples, wt %

Sample	F	SiO_2	P_2O_5	CaO	$HREE_2O_3$	$LREE_2O_3$	ThO_2	UO_2	Σ
65863 light (1, 3, 5)[1]	1.5	20.1	3.1	15.3	n.d.	47.5	2.1	1.0	90.6
dark (2, 4)	1.8	19.7	4.0	16.8	1.3	45.4	1.8	n.d.	90.8
1769 light (2, 6)	4.3	24.3	3.9	16.1	n.d.	50.2	1.3	″	100.1
dark (1, 4, 5)	4.7	23.4	4.6	18.4	1.8	45.1	1.6	″	99.6
89510 light (1, 2, 4)	2.3	21.5	n.d.	15.9	36.0	7.6	1.2	″	87.4[2]
dark (3, 5)	2.4	20.8	″	14.4	33.1	5.4	1.3	″	80.5[3]
1775 light (6, 7, 9)	1.6	20.4	2.5	16.5	1.1	36.9	11.2	1.1	91.3
dark (4, 5, 8)	1.9	20.1	3.2	17.2	n.d.	37.4	11.0	1.0	91.8
1771 light (1, 2, 5)	1.5	19.9	2.8	16.1	5.7	34.1	4.6	0.7	85.4
dark (3, 4)	1.8	19.6	3.7	17.2	5.5	36.6	3.9	n.d.	88.3
62388 dark (3, 4, 7)	3.2	22.0	3.5	18.9	n.d.	35.1	12.1	″	94.8
light (1, 2, 5, 6)	3.0	22.4	3.1	19.0	″	37.9	13.8	″	99.2

Notes: [1] Point numbers in Fig. 1. [2] 0.9 wt % Al_2O_3, 1.2 wt % MnO, and 0.8 wt % FeO were also determined. [3] 1.0 wt % Al_2O_3, 1.3 wt % MnO, and 0.8 wt % FeO were also determined.

Other britholite samples demonstrate less distinct zoning. Domains lighter than the groundmass are discernible in samples Bt-8, 1775, 1769, and 65863, but the contrast in color is less than in the other samples. Such domains are 50–150 μm in size and chaotically arranged. The light and dark domains in samples Bt-8, 1775, and 1769 differ in CaO content; in sample 65863, they vary in REE_2O_3 contents as well.

Based on the area-averaged compositions, the formulas of britholites have been calculated (Table 3). The formulas of samples 89510 and 62388 are based on the average compositions of light zones only, which likely

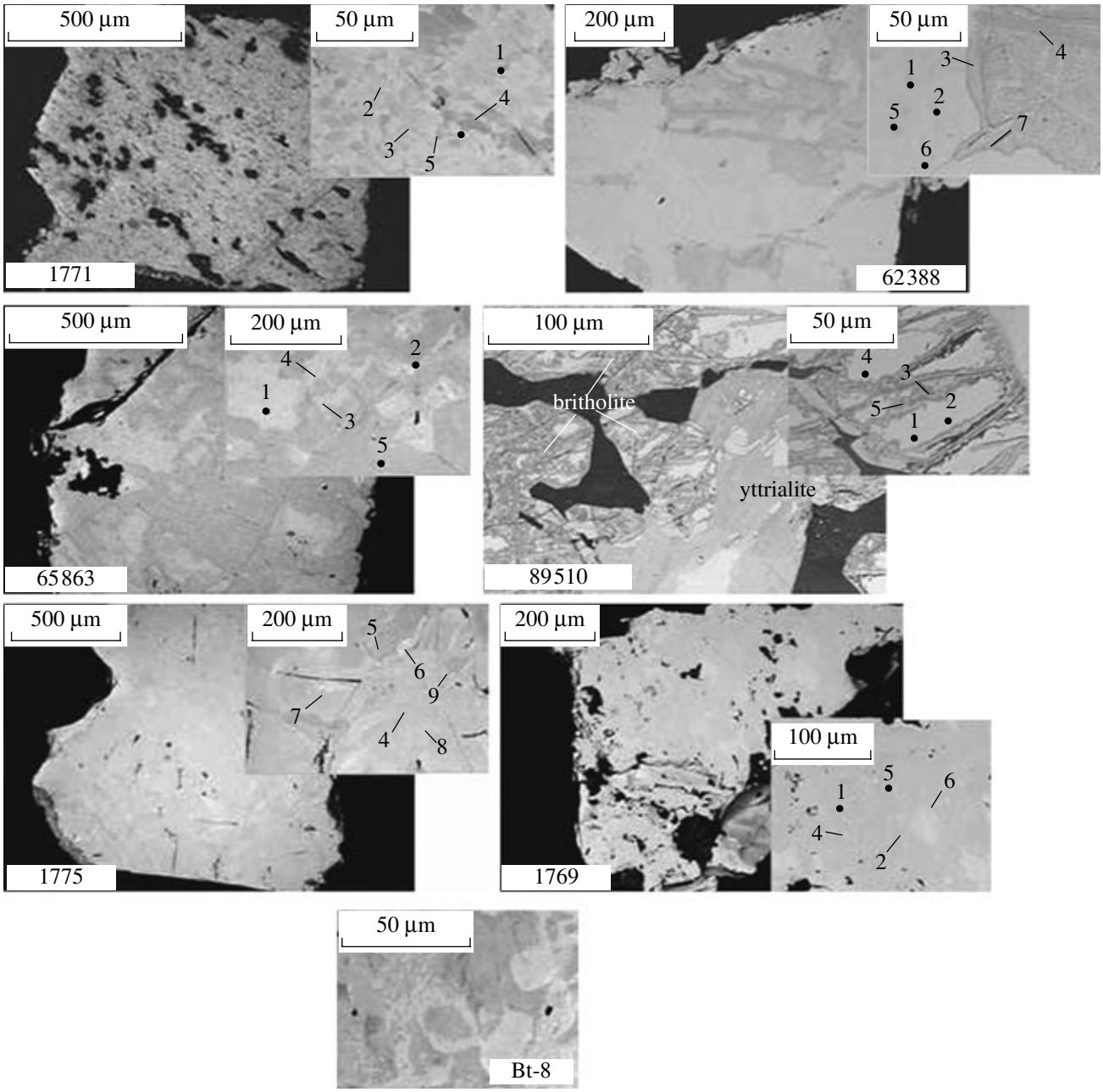

Fig. 1. BSE images of selected areas of samples 1771, 89510, and Bt-8 (bar, 50 μm) and 1769, 1775, and 65863 (bar, 200 μm). (1–9) Numbers of SEM/EDS analyses in Table 2.

correspond to unaltered britholite. According to the general britholite formula $[(^{VII}A,^{IX}A)_{10}{}^{IV}B_6O_{24}(F^-,OH^-)_2]$, where A = Ca^{2+}, REE^{3+}, or Th^{4+} (the main cations) and B = $Si^{4+} + P^{5+} + B^{5+} + Al^{3+}$, the calculation was carried out for a sum of cations at site B equal to 6. This method of formula calculation yields a deficiency in cations occupying site A in all examined britholite samples except 89510: the sum of atoms in the formulas ranges from 8.12 to 9.73, whereas the theoretical value equals 10.

Structural characteristics. The britholite structures were studied using X-ray patterns and electron diffraction patterns. X-ray patterns indicate the general state of the crystalline structure of minerals and allow the crystallinity of a sample versus its amorphism to be estimated. Samples with undisturbed primary structures are usually characterized by X-ray patterns with distinct and narrow high-intensity peaks. As the structure is destroyed under the α decay of radioactive components, the peaks become less intense and wider. X-ray patterns of amorphous samples are devoid of any

Table 3. Calculated formulas of minerals

Sample	Formula
65863	$(Ca_{4.09}Ce_{1.94}La_{1.40}Nd_{0.31}Y_{0.16}Th_{0.11}Pr_{0.10}U_{0.01})(Si_{4.99}P_{1.01})O_{21.92}F_{1.55}$
1769	$(Ca_{4.54}Ce_{2.78}La_{1.03}Y_{0.22}Th_{0.07}U_{0.03})(Si_{4.88}P_{1.12})O_{21.48}F_{3.75}$
Bt-8	$(Ca_{4.61}Ce_{2.57}La_{1.00}Nd_{0.98}Th_{0.26}Pr_{0.16}Sm_{0.09}Eu_{0.04}U_{0.02})(Si_{5.29}P_{0.71})O_{23.44}F_{3.29}$
89510	$(Ca_{4.53}Y_{4.29}Ce_{0.36}Mn_{0.27}Dy_{0.25}Er_{0.23}Fe_{0.18}Nd_{0.15}La_{0.15}Th_{0.07})(Si_{5.72}Al_{0.28})O_{24.45}F_{1.94}$
1775	$(Ca_{4.69}Ce_{1.74}La_{1.15}Th_{0.65}Nd_{0.35}Y_{0.11}Pr_{0.11}Sm_{0.07}U_{0.05})(Si_{5.28}P_{0.72})O_{23.02}F_{1.55}$
1771	$(Ca_{4.83}Ce_{1.74}Nd_{0.99}Y_{0.86}La_{0.64}Th_{0.26}Pr_{0.15}Sm_{0.12}U_{0.04})(Si_{5.20}P_{0.80})O_{23.8}F_{1.52}$
62388	$(Ca_{4.89}Ce_{1.84}La_{1.09}Th_{0.75}Nd_{0.3}Pr_{0.11})(Si_{5.31}P_{0.69})O_{22.6}F_{2.28}$

Table 4. ThO_2 and UO_2 contents and calculated irradiation doses for the studied britholites, wt %

Sample number (age in years)	UO_2	ThO_2	$D \times 10^{19}$, α decays/g	D, displacements/atom	Structure
65863 (3.2×10^8)	0.2	2.0[1] (1.5–2.7)[2]	0.6 (0.3–1.5)	0.5 (0.3–1.3)	Partly crystallized
1769 (15×10^8)	0.6	1.3 (0.9–2.1)	1.4 (1.0–2.2)	1.2 (0.8–1.9)	″
Bt-8 (3.2×10^8)	0.3	4.1 (3.0–5.3)	0.9 (0.6–1.0)	0.8 (0.5–0.9)	Entirely amorphous
89510 (26×10^8)	n.d.	1.2 (0.8–2.3)	2.3 (1.5–4.3)	1.8 (1.2–3.5)	″
1775 (3.2×10^8)	0.8 (0.2–1.2)	11.1 (9.8–12.1)	3.2 (2.3–3.7)	2.8 (2.1–3.4)	″
62388 (3.0×10^8)	n.d.	13.8 (11.5–14.2)	2.8 (2.4–2.9)	2.4 (2.0–2.5)	″
1771 (26×10^8)	0.6	4.3 (3.8–4.6)	8.1 (7.2–8.7)	6.9 (6.1–7.4)	″

Notes: [1] Average value. [2] Range.

peaks. Electron diffraction patterns allow, in turn, the structure of small (fractions of a micrometer) domains of a sample to be examined.

Figure 2 demonstrates two types of X-ray patterns obtained for britholites and, for comparison, the X-ray pattern and electron diffraction pattern of the britholite crystalline structure recovered by annealing. The first type of X-ray patterns (samples 65863 and 1769) is characterized by wide, low-intensity peaks in the region of the main britholite reflections (211), (112), and (120). The X-ray patterns of the second type (in the remaining samples) are devoid of peaks. The examined samples also differ in the patterns of electron microdiffraction: both (1) poorly expressed dotty and (2) ring (a wide halo around the central reflection of the electron beam) patterns are recognized. Some samples demonstrate electron diffraction patterns of both types, probably, due to a nonuniform distribution of radioactive elements and a variable degree of amorphization.

In the samples characterized by X-ray patterns with low peaks and dotty electron diffraction patterns, the content of radioactive components (ThO_2 + UO_2) amounts to 2 wt %, while in the remaining samples it exceeds 4.5 wt %. The exception is spencite in sample 89510, which is devoid of uranium and contains 1.2 wt % thorium oxide.

Calculation of the irradiation dose. Based on the thorium and uranium concentrations and the age of samples, the accumulated irradiation doses (D, α decays/g) of britholites have been calculated (Table 4) from the equation derived by Lumpkin and Chakoumakos (1988):

$$D = 8 \times {}^{238}N(e^{\lambda_{238}t} - 1) + 6 \times {}^{232}N(e^{\lambda_{232}t} - 1),$$

where ${}^{238}N$ and ${}^{232}N$ are the ThO_2 and UO_2 contents (quantity of molecules per gram); λ_{232} and λ_{238} are the decay constants of ^{232}Th and ^{238}U (yr^{-1}); t is the age (yr); and 6 and 8 are the numbers of α-particles formed from the decay of a thorium and a uranium atom, respectively. The accumulated irradiation dose depends on both the content of radioactive elements in the mineral and its age.

In order to compare the obtained results with data on ion irradiation of synthetic compounds, the doses measured in α decays/g units were recalculated into displacements per atom in line with the equation (Lumpkin and Chakoumakos, 1988):

$$D(\text{displacements/atom}) = \frac{1500DM}{N_f N_A},$$

where D is the irradiation dose (α decays/g), M is the molecular mass of the compound (g), N_f is the number of atoms in the compound formula, and N_A is Avogadro's number.

According to the XRD and TEM data, sample 65863, with a partly metamict structure, is characterized by an accumulated irradiation dose of 0.6×10^{19} α decays/g (0.5 displacements/atom), while this parameter in the

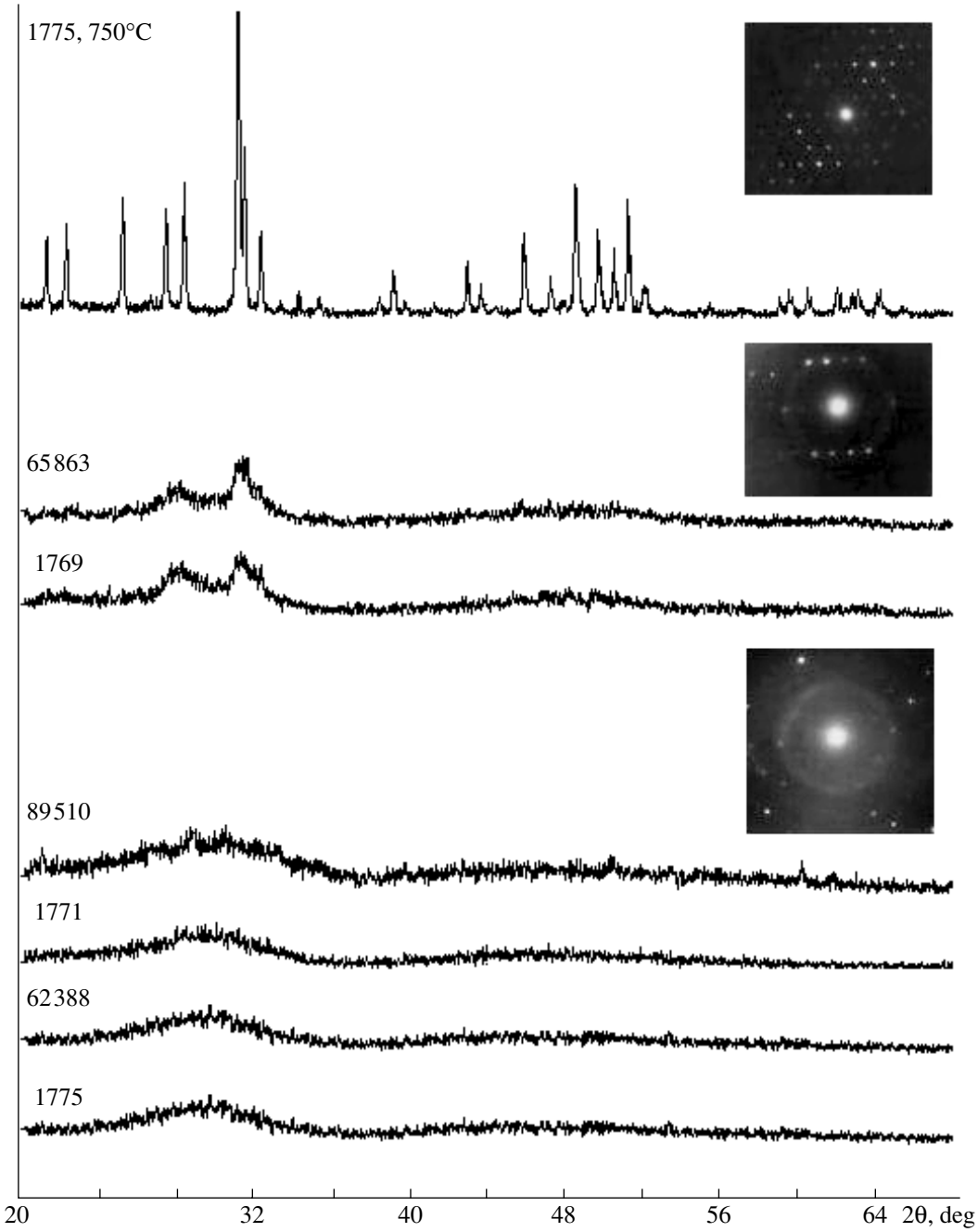

Fig. 2. Types of X-ray patterns and the corresponding electron diffraction patterns of britholites.

entirely amorphous samples Bt-8, 89510, 1775, 62388, and 1771 varies from 0.9×10^{19} to 8.1×10^{19} α decays/g (0.8–6.9 displacements/atom).

The XRD and TEM data (Fig. 2) indicate that the britholite structures in samples 1769 and Bt-8 have been retained to a certain degree. Sample 1769, 15.0×10^8 yr in age and with an accumulated irradiation dose of 1.2 displacements/atom, has a partly metamict structure, while sample Bt-8, 3.2×10^8 yr in age and with an accumulated irradiation dose of 0.8 displacements/atom, exhibits an entirely amorphous structure. This could be caused by a partial loss of radioactive elements by sample Bt-8 due to its secondary alteration and, hence, a reduced accumulated irradiation dose, but the SEM examination indicates that this was not the case: no substantial changes in the sample surface or chemical variations are observed. The variable retention of the lattice inconsistent with accumulated irradiation doses is most likely caused by recovery of the structure owing to annealing of sample 1769. The behavior of minerals

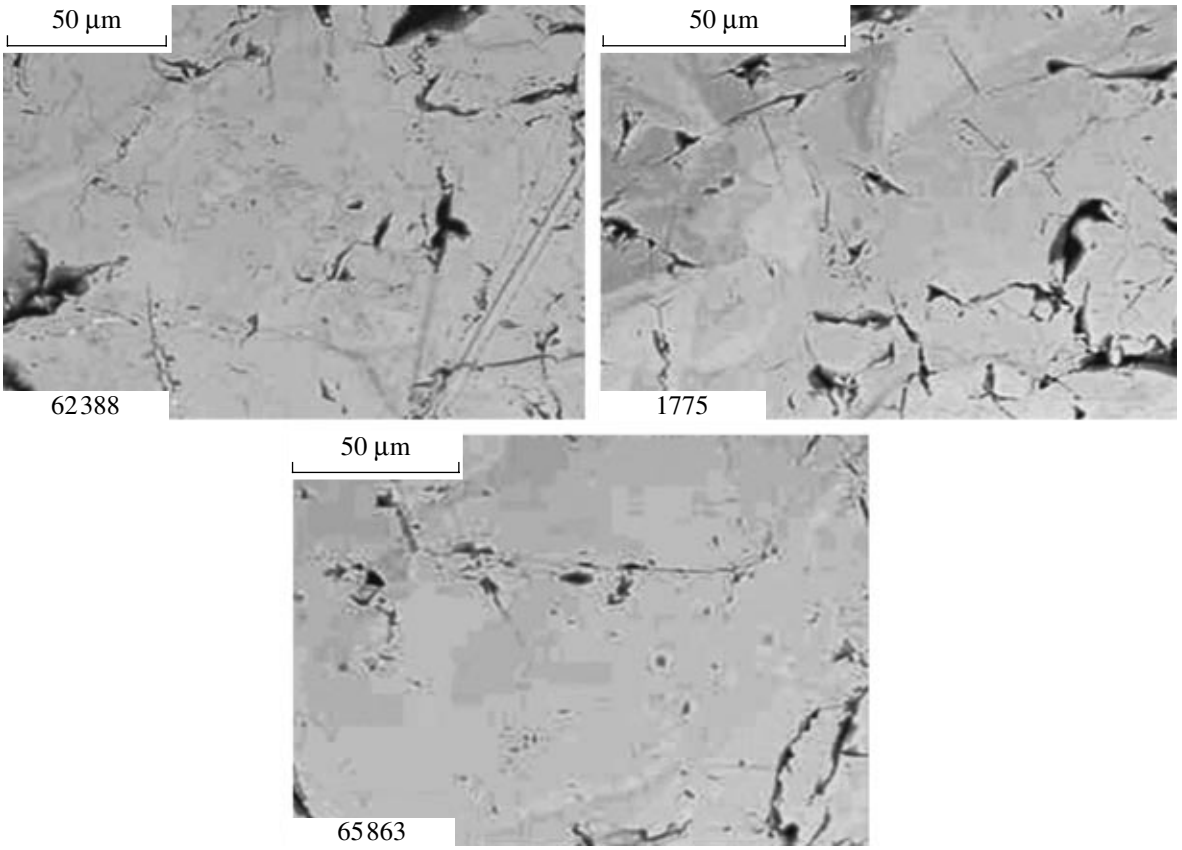

Fig. 3. BSE images of annealed samples 62388, 1775, and 65863.

during annealing was studied in order to ascertain the effect of temperature on lattice stability.

Structure recovery by annealing. Along with irradiation-induced destruction of the crystalline lattice in minerals, recovery of the structure owing to heating may occur.

To confirm the initial apatite-type structure of metamict minerals, samples 65863, 1775, 62388, and Bt-8 were annealed at 750°C for 6 h. As was indicated by the XRD data, the apatite-type lattice was recovered in all samples. No newly formed phases appeared after annealing. As can be seen from BSE images (Fig. 3), the annealed samples 1775 and 62388 retained their initial zonal patterns, while samples Bt-8 and 65863 lost these patterns. At the same time, the zonal patterns of the first two samples were less distinct than they were before the annealing. The chemical composition of samples was determined after the heat treatment. According to SEM data, annealed samples 1775 and 65863 lost their fluorine (Table 5).

The dynamics of the structure recovery in samples 1775, 65863, and Bt-8 was studied with DTA. The thermal curves of britholites from samples 65863 and 1775 at a temperature of approximately 200°C show an insignificant endothermic peak probably related to dehydration of the mineral. This is indicated by the mass loss on ignition, which is approximately 1 wt % for each sample. The curve obtained for sample Bt-8 demonstrates a single exothermic peak related to the recovery of the destroyed structure. The mass loss on

Table 5. Compositions of samples, wt % before and after annealing at 750°C for 6 h

Sample	F^-	SiO_2	P_2O_5	CaO	ΣY_2O_3	ΣCe_2O_3	ThO_2	UO_2
65863	2.0[1]/n.d.[2]	20.4/20.7	4.9/4.2	15.6/16.7	1.2/1.2	41.9/43.0	2.0/1.8	0.2/0.3
Bt-8	3.7/3.1	18.8/20.3	3.0/3.7	15.3/15.9	1.3/1.2	47.3/48.9	4.1/4.2	0.3/0.3
1775	1.9/n.d.	20.5/19.4	3.3/3.2	17.0/16.6	0.8/n.d.	36.7/37.1	11.1/10.3	0.8/1.0
62388	3.0/2.8	20.3/20.8	3.4/3.9	19.5/19.7	″	37.9/36.9	13.8/13.3	n.d.

Notes: [1] Before annealing. [2] After annealing.

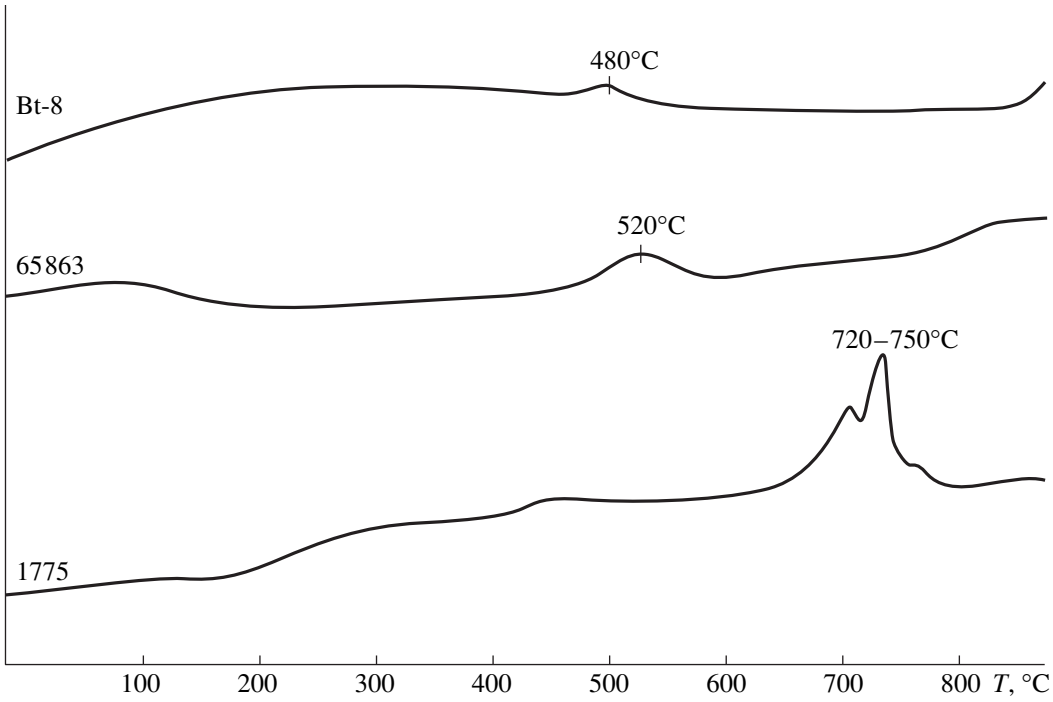

Fig. 4. Thermal curves for samples Bt-8, 1775, and 65863.

ignition was 2 wt %. Recrystallization of amorphous samples (the exothermic peaks on heating curves) occurs at temperatures of 480 (Bt-8), 520 (65863), and 750°C (1775) (Fig. 4). The difference in the temperatures at which the mineral structure is recovered is most likely related to a different degree of their structural amorphization. For example, britholite from sample 1775, with the maximal $ThO_2 + UO_2$ content (approximately 12 wt %) and an age of 3.2×10^8 yr, has an entirely amorphous structure as indicated by the X-ray pattern. The content of radioactive elements in samples 65863 and Bt-8, which have a similar age of 3.2×10^8 yr, is approximately 2 and 4 wt %, respectively. The structures of these minerals are less destroyed, and, therefore, they were recovered at a lower temperature than sample 1775.

Taking into account the DTA data, seven annealing temperatures were selected for the detailed study of the recrystallization of sample 1775: 100, 300, 500, 550, 600, 750, and 800°C (Fig. 5). After annealing at each of these temperatures, the degree of structure recovery was established with XRD. During annealing for 5 h, the recrystallization begins in the interval 300–500°C and the main phase of the structure recovery occurs in the interval 500–600°C. A further increase in the temperature does not lead to substantial changes in diffraction patterns. An insignificant shift of the main britholite reflection (211) toward larger angles, along with a decrease in d_{211} from 2.840 to 2.829 Å, is observed only in the temperature range 600–750°C. This testifies to a decrease in the unit cell parameter of britholite at the final stage of structure recovery.

In order to establish the correlation between the mineral recrystallization rate and annealing duration, the sample was additionally heated at 500°C for 8 h. No differences in X-ray patterns for the samples heated for 5 and 8 h were revealed.

DISCUSSION

Dynamics of structure recovery by annealing. Proshchenko et al. (1972) studied the recovery of the structure of metamict britholite by annealing for a sample taken from the northern Baikal region. The chemical composition of the mineral is close to that of sample 1775: for example, the ThO_2 content in both samples amounts to 11 wt % (Glushchenko and Li, 1966) (Table 1). In the DTA curve, the main exothermic peak reflecting the structure recovery is observed at 760°C (750°C in sample 1775). Taking into account previous DTA data, the mineral charges were annealed for 30 and 60 min at 500, 700, 720, 785, 800, and 900°C. The diffraction patterns obtained for the samples annealed for different times but at the same temperature are identical. According to XRD data, the recovery of the structure (the appearance of the first low-intensity peaks) begins at 700°C. At the same time, according to the authors (Proshchenko et al., 1972), the first indications of mineral recrystallization were observed in transmitted light under an optical microscope already after annealing at 500°C. This was expressed in a weak

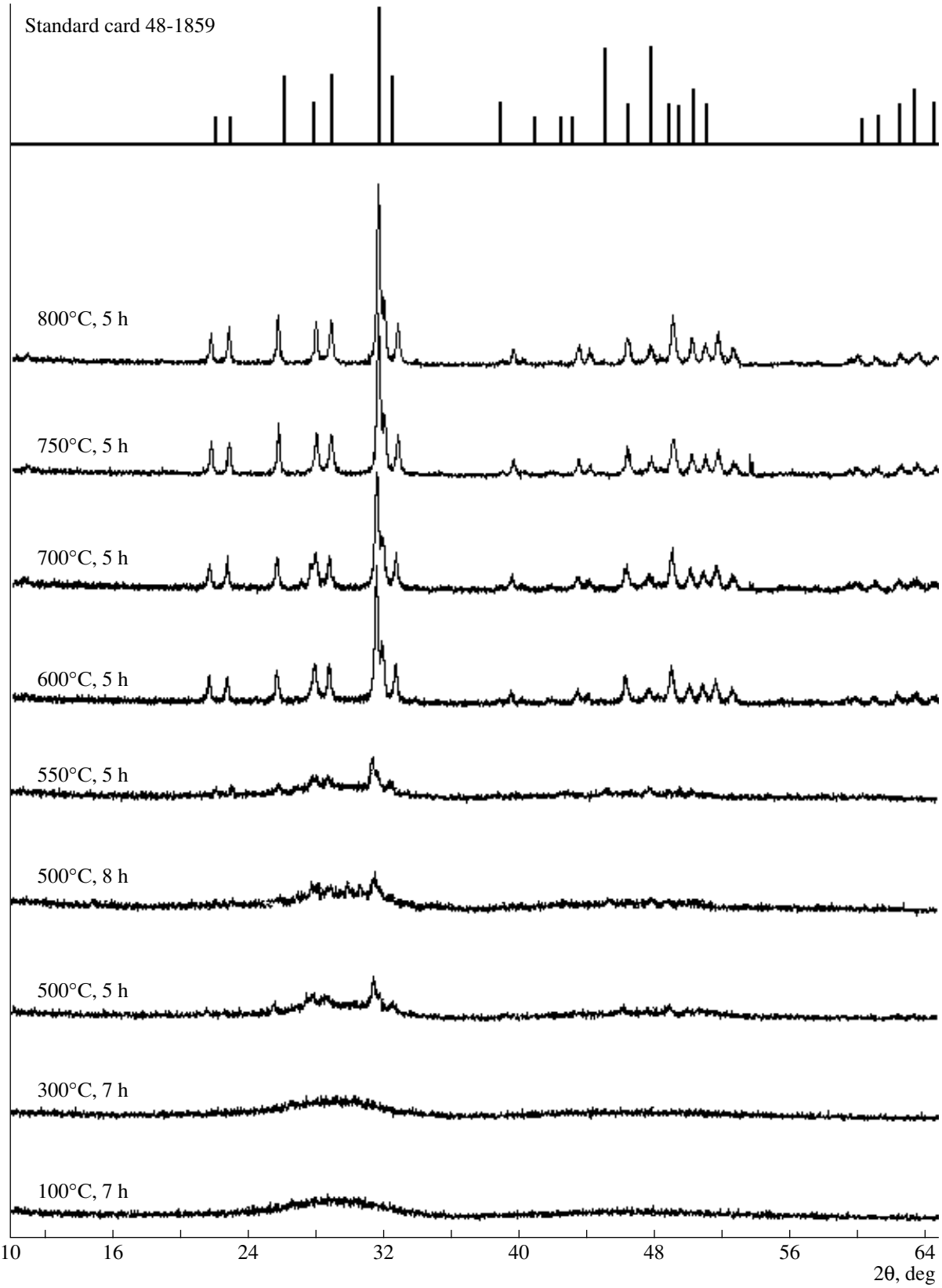

Fig. 5. X-ray patterns of sample 1775 recording successive recovery of the structure with increasing temperature.

Table 6. Radiation stability of natural and synthetic britholites

Sample	Irradiation type	D_c, displacements/atom	T_c, °C	Source
Natural britholites	^{232}Th, U	0.8	–	Author's data
Natural britholite	^{232}Th	1	–	Gong et al., 1997
$(Ca, REE, Mg, Th)_{10}$				
$((Si, P)_4O_6)(O, OH, F)_2$				
Synthetic britholite	^{244}Cm,	0.2	550	Weber and Ewing, 2002
$Ca_2Nd_8(SiO_4)_6O_2$	^{238}Pu	0.2		
Synthetic britholite	Ne^+	0.3–0.5	87	Ewing et al., 1995
$Ca_2La_8(SiO_4)_6O_2$	Kr^+	0.3–0.5	437	
Synthetic britholite				Utsunomiya et al., 2003
$Ca_4(Gd, Ce)_6((Si, Fe)O_4)_6O_2$	Kr^{2+}	0.15	607	
$Ca_4(Nd, Ce, La, Zr, Eu, Fe)_6(SiO_4)_6O_2$	Xe^+	0.15	737	

Note: D_c is the critical irradiation dose; T_c is the critical temperature.

anisotropy acquired by some domains of the sample, which became distinct at 700°C. In the temperature interval 725–785°C, X-ray patterns exhibit all the peaks characteristic of the apatite-type structure, which become more distinct and narrower with increasing temperature. A granular structure is observable under a microscope: large anisotropic well-faceted grains are incorporated into a partly isotropic groundmass. The authors of this publication noted that recrystallization of the initially amorphous mineral is completed within the temperature interval indicated above. At 800 and 900°C, individual grains merge and britholite becomes entirely anisotropic.

In the present study, it was found that, when the duration of annealing is increased to 5 h, the recrystallization of an amorphous sample of the same composition is recorded in the X-ray pattern already at 500°C and the main stage of structure recovery falls within the interval 550–600°C. Thus, the data of this study combined with the results reported by Proshchenko et al. (1972) demonstrate the obvious dependence of the structure recovery temperature on the duration of annealing.

In the case of real wastes, it may be assumed that a significant duration of their underground disposal and an inferred temperature of approximately 50°C in containers with solidified actinide HLW (Marples, 1996) will slow down the radiation-induced destruction of the structure, favoring the retention of the natural properties of confinement matrices.

Comparison of radiation stability of britholites obtained with different methods. Previous studies on the radiation stability of synthetic compounds with the apatite-type structure have been carried out mainly with two methods: heavy ion irradiation or implantation of short-lived ^{244}Cm and ^{238}Pu isotopes into the phase structure (Table 6). Different stages of structural amorphization have been reached by increasing the duration of experiments. Owing to different composition of samples and types (masses) of ions, the method of ion irradiation yielded wide ranges of critical doses and temperatures. Structural amorphization of synthetic phases with the apatite-type structure occurs under an accumulated irradiation dose varying from 0.15 displacements/atom (irradiation with Kr^+ and Xe^+) (Utsunomiya et al., 2003) to 0.5 displacements/atom (irradiation with Ne^+) (Ewing et al., 1995). The critical temperature ranges from 87°C (irradiation with Ne^+) (Ewing et al., 1995) to 737°C (irradiation with Xe^{2+}) (Utsunomiya et al., 2003). The critical irradiation dose on implantation of short-lived ^{244}Cm and ^{238}Pu isotopes into the phase structure at 25°C is approximately 0.2 displacements/atom and the critical temperature equals 550°C (Weber and Ewing, 2002).

Gong et al. (1997) studied the radiation stability of a single sample of natural britholite with nonuniform distribution of radioactive elements. The chemical composition of britholite was determined in domains with a varying degree of structural damage, which were selected from electron microdiffraction patterns; doses of irradiation were calculated for particular domains. When studying zonal britholite and other structural types of this mineral, Ewing et al. (1995) defined stages with a partly crystalline, partly amorphous, and entirely metamict lattice. An irradiation dose below 0.3 displacements/atom ($\approx 4 \times 10^{18}$ α decays/g) corresponds to the stage with an almost undisturbed structure; approximately 0.5 displacements/atom ($\approx 6 \times 10^{18}$ α decays/g), to the stage with a partly amorphous structure; and ~1 displacements/atom ($>10^{19}$ α decays/g), to the stage of an entirely metamict structure.

The initial amorphization stage in the examined britholites was not observable because of the high value of the accumulated irradiation dose. The X-ray pattern inherent to the initial stage was obtained for sample 1775 annealed at a temperature of 600°C (Fig. 5). This stage

is also characterized by the X-ray pattern obtained by Proshchenko et al. (1972) for the sample annealed at 785°C. The stage of partial structural damage is exemplified in samples 65863 and 1769 at an accumulated irradiation dose that amounts to 0.5 displacements/atom. The complete amorphization of the examined britholites occurs at an accumulated irradiation dose that exceeds 0.8 displacements/atom (0.9×10^{19} α decays/g), as is observed in samples Bt-8, 1775, 1771, 89510, and 62388.

The published critical irradiation doses for synthetic silicates with the apatite-type structure are two to five times lower than for natural britholites. This is related, first, to different methods of sample irradiation and, second, to a partial recovery of the mineral structure over geologic time. The partial recovery of the structure is confirmed by the study of other radioactive minerals. It has been shown that the critical irradiation dose increases by two to three times when a temperature of 100–200°C is maintained over a long geologic time (Lumpkin, 2001).

Calculations of the accumulated irradiation doses for crystalline HLW matrices indicate that ceramics containing 20 wt % ^{239}Pu will accumulate a dose of 10^{19} α decays/g over 10^3 yr (Weber et al., 1997). In the case of another composition and content of radioactive components, the rate of irradiation dose accumulation will be different. For example, Synroc ceramic contains 20 wt % HLW components including 0.1 wt % Am_2O_3 + Cm_2O_3, approximately 0.4 wt % NpO_2, 0.004 wt % PuO_2, and 0.7 wt % U_3O_8 (Ringwood, 1985) will receive an irradiation dose of 10^{19} α decays/g over 10^5 yr (*Radioactive*…, 1988).

The radioactive damage of matrix phases with britholite structure is close to the processes that proceed in natural U- and Th-bearing minerals. Therefore, their critical irradiation doses will be close to the values for natural britholites. This implies that, as in natural samples, the recovery of the structure with time is also possible for synthetic matrices.

CONCLUSIONS

Seven minerals of the britholite group from 3.2×10^8 to 26×10^8 years in age containing 1.4–14 wt % ThO_2 + UO_2 have been studied with XRD, SEM/EDS, TEM, and DTA. The XRD and TEM results fixed the stages of partial and complete destruction of the structure.

The complete amorphization of the britholite lattice occurs under an accumulated irradiation dose of 0.9×10^{19} α decays/g (0.8 displacements/atom). A ceramic with 20 wt % ^{239}Pu will accumulate a similar irradiation dose over 10^3 yr, while 10^5 yr are required for Synroc ceramic with 20 wt % HLW to accumulate the same dose. The critical irradiation dose of natural britholites is higher than that of synthetic compounds. This is caused largely by thermal recovery of the mineral structure through geologic time.

The annealing of four metamict samples at a temperature of 750°C for 5 h resulted in recovery of apatite-type structures. The comparison of the obtained results with published data on samples annealed for 0.5–1.0 h shows that the rate of structure recovery increases with the duration of annealing. For example, the recrystallization of a metamict sample containing approximately 11 wt % ThO_2 occurs at 800–750°C in 1.0–1.5 h, while an increase in the heating duration to 5–8 h reduces the recrystallization temperature to 600–550°C.

Based on the results obtained from the study of radioactive minerals, it may be suggested that a significant storage time for solidified HLW will promote a slowing of irradiation-induced destruction of matrices with the apatite-type structure at temperatures similar to those maintained in underground storages. In this case, the phases with the apatite-type structure will retain the lattice and its stability over a longer time and thus prevent actinides from migration to the environment.

ACKNOWLEDGMENTS

I thank A.R. Alimova for kindly placing samples at my disposal and L.A. Kochetkova, A.V. Sivtsov, and O.R. Rafal'skaya for performing analytical procedures. This study was supported by the Federal Agency for Science and Innovations (state contract no. 02.434.11.4007) and the Russian Foundation for Basic Research (project no. 05-05-64094).

REFERENCES

1. O. A. Belyaev, F. P. Mitrofanov, T. B. Bayanova, et al., "The Late Archean Age of Acid Metavolcanic Rock in the Lesser Keivy, Kola Peninsula," Dokl. Akad. Nauk **379** (5), 651–654 (2001) [Dokl. Earth Sci. **379A** (6), 705–708 (2001)].
2. V. V. Chuprov, "Accessory Minerals of the Kharitonovsky Alkaline Massif," Zap. Vseross. Mineral. O–va **101** (4), 430–437 (1972).
3. R. C. Ewing, "The Design and Evaluation of Nuclear-Waste Forms: Clues from Mineralogy," Can. Mineral. **39**, 697–715 (2001).
4. R. C. Ewing, W. J. Weber, and F. W. Clinard, "Radiation Effects in Nuclear Waste Forms for High-Level Radioactive Waste," in *Progress in Nuclear Energy* (1995), Vol. 29, pp. 63–127.
5. A. A. Glushchenko and A. F. Li, "Britholite from an Alkaline Massif in the Northern Baikal Region," Proc. Irkutsk State Research Institute of Rare and Nonferrous Metals, No. 14, 100–107 (1966).
6. W. L. Gong, L. M. Wang, R. C. Ewing, et al., "Transmission Electron Microscopy Study of α-Decay Damage in Aeschynite and Britholite," in *Proceedings of Symposium on Scientific Basis for Nuclear Waste Management XX* (MRS, Pittsburgh, 1997), Vol. 465, pp. 649–656.

7. I. I. Kupriyanova, G. A. Sidorenko, and M. A. Kudrina, "Minerals of Britholite Group," in *Geology of Rare-Element Deposits. Rare Earth Silicates* (Nedra, Moscow, 1966), No. 26, pp. 23–66 [in Russian].
8. G. R. Lumpkin, "Alpha-Decay Damage and Aqueous Durability of Actinide Host Phases in Natural Systems," J. Nucl. Mater. **289**, 136–166 (2001).
9. G. R. Lumpkin and B. C. Chakoumakos, "Chemistry and Radiation Effects of Thorite-Group Minerals from the Harding Pegmatite, Taos Country, New Mexico," Am. Mineral. **73**, 1405–1419 (1988).
10. J. A. C. Marples, "Vitrification of Plutonium for Disposal," in *Disposal of Weapon Plutonium* (Kluwer Acad. Publ. 1996), pp. 179–195.
11. S. V. Nechaev and S. G. Krivdyuk, "Spatial Distribution of Alkaline Rocks in the Ukrainian Shield," Geol. Zh., No. 3, 113–120 (1989).
12. *Phosphate Glasses with Radioactive Waste*, Ed. by A. A. Vashman and A. S. Polyakov (TSNIIAtominform, Moscow, 1997) [in Russian].
13. E. G. Proshchenko, I. D. Belyaeva, S. I. Lebedeva, and E. B. Khalezova, "Mechanism of Metamict Britholite Crystallization as a Result of Heating," Mineral. Sb. **26** (3), 306–312 (1972).
14. *Radioactive Waste Forms for the Future* (Elsevier, New York, 1988).
15. A. E. Ringwood, "Disposal of High-Level Nuclear Wastes: A Geological Perspective," Mineral. Mag. **49**, 159–176 (1985).
16. P. B. Rose, M. I. Ojovan, N. C. Hyatt, and W. E. Lee, "Crystallization within Simulated High Level Waste Borosilicate Glass," in *Proceedings of Symposium on Scientific Basis for Nuclear Waste Management XXVIII* (MRS, Warrendale, 2004), Vol. 824, pp. 321–3260.
17. T. V. Smelova, N. V. Krylova, S. V. Yudintsev, and B. S. Nikonov, "Silicate Matrix of Actinide-Bearing Wastes," Dokl. Akad. Nauk **374** (2), 242–246 (2000) [Dokl. Earth Sci. **374** (7), 1149–1152 (2000)].
18. C. G. Sombret, "Waste Forms for Conditioning High-Level Radioactive Solutions," in *Geol. Disposal of High-Level Radioactive Wastes* (Theoph. Publ, Athens, 1987).
19. S. Utsunomiya, S. Yudintsev, L. M. Wang, and R. C. Ewing, "Ion Beam and Electron Beam Irradiation of Synthetic Britholite," J. Nucl. Mater. **322**, 180–188 (2003).
20. W. J. Weber, R. C. Ewing, C. A. Angell, et al., "Radiation Effects in Glasses Used for Immobilization of High-Level Waste and Plutonium Disposition," J. Mater. Res. **12** (8), 1946–1975 (1997).
21. W. J. Weber and R. C. Ewing, "Radiation Effects in Crystalline Oxide Host Phases for the Immobilization of Actinides," in *Proceedings of Symposium on Scientific Basis for Nuclear Waste Management XXVI* (MRS, Warrendale, 2002), Vol. 713, pp. 443–454.
22. D. Zhao, L. Li, L. L. Davis, et al., "Gadolinium Borosilicate Glass-Bonded Gd-Silicate Apatite: A Glass-Ceramic Nuclear Waste Form for Actinides," in *Proceedings of Symposium on Scientific Basis for Nuclear Waste Management XXIV* (MRS, Warrendale, 2001), Vol. 556, pp. 199–206.
23. A. Ya. Zhidkov, S. L. Mirkina, and M. N. Golubchina, "Absolute Age of Alkaline and Nepheline Syenites in the North Baikal Highland," Dokl. Akad. Nauk SSSR **149** (1), 152–155 (1963).